RSC Advances

PAPER

View Article Online
View Journal | View Issue

Cite this: *RSC Adv.*, 2015, **5**, 43965

Enhanced therapeutic efficacy and cytotoxicity of doxorubicin-loaded vitamin E – Pluronic micelles against liver cancer

Y. J. Li,* M. Dong, F. M. Kong and J. P. Zhou

In this study, a new polymeric micelle delivery system was developed to increase the therapeutic efficacy of doxorubicin (DOX) and to reduce its associated side effects. For this purpose, DOX-loaded Pluronic-alpha-tocopheryl succinate polymeric micelles (P/TOS-DOX) were successfully prepared for the therapeutic treatment of hepatocellular carcinoma. We show that the drug-loaded micelles exhibit typical pH-dependent and sustained drug release profile. These micelles were nanosized, around ~100 nm, with spherical morphology. The micelles were predominantly distributed in the cytoplasmic region, which facilitates the cancer-killing potency of the chemotherapeutic drug. The IC_{50} value of DOX and P/TOS-DOX remained at 1.18 μg ml^{-1} and 0.72 μg ml^{-1}, respectively, indicating significant inhibition of cancer cell proliferation by the micellar carrier. Micellar incorporation of the drug effectively shielded it from elimination and subsequently prolonged the blood circulation and half-life of the anticancer drug. P/TOS-DOX accumulated preferentially in the tumor immediately after systemic administration, and a significant proportion of the drug was observed by the end of 24 h. Especially, P/TOS-DOX exhibited superior tumor growth inhibition compared to that in the free DOX-treated group. More importantly, the side effects of DOX were effectively decreased when it was administered using micellar carriers. Overall, our results suggest that P/TOS-DOX could be an attractive carrier in the therapeutic approach to hepatocellular carcinoma.

Received 6th March 2015
Accepted 16th March 2015

DOI: 10.1039/c5ra04027b

www.rsc.org/advances

Introduction

Liver cancer, or hepatocellular carcinoma (HCC), is one of the most widespread and lethal cancers in the world. It is the third most common cause of cancer-related death.[1] Each year, the number of deaths due to HCC increases, especially in developing countries like China. In the United States alone, nearly 20 000 patients died, with 25 000 new cases identified in 2012.[2,3] At present, chemotherapy-based single or dual drug regimen is the main treatment option. However, conventional chemotherapy often suffers from non-specific targeting, non-specific mode of action, and high adverse effects, which often hinder its clinical success rate.[4] Besides, one of the major problems associated with cancer chemotherapy is the difficulty in maintaining the therapeutic drug concentration in the tumor site for the desired period of time.[5,6]

To overcome the limitations associated with chemotherapeutic drugs, various drug delivery systems have been developed to improve the delivery and to reduce the side effects.[7] The nanoparticulate delivery system could potentially avoid the reticuloendothelial system (RES) and help prolong the half-life of drugs in the body and in blood circulation. Moreover, nanoparticles less than 200 nm could passively target cancer tissues *via* the enhanced permeability and retention (EPR) effect.[8–10] Although many polymeric nanoparticles have been designed, the quest to prepare novel nanocarriers remains.

In this regard, amphiphilic block copolymer-based polymeric micelles have attracted significant attention from researchers worldwide.[11] The prime advantages with polymeric micelles are their small particle size, high drug loading capacity, long blood circulation time, good biodistribution, and lower side effects.[12] Especially, Pluronic block copolymers, which consist of hydrophilic poly(ethylene oxide) (PEO) and hydrophobic poly(propylene oxide), have favorable properties.[13] Pluronic polymers are reported to circumvent multidrug resistance (MDR) and increase the potency of anticancer drugs. Besides, hydrophilic PEO could effectively prolong the blood circulation time by virtue of its antifouling characteristics.[14] However, the low drug loading capacity and instability of Pluronic micelles in the systemic environment or in circulation (due to a lack of structural integrity) limit its further use.[15] Alpha-tocopheryl succinate (α-TOS), a well-known vitamin E analogue, can be used as a hydrophobic segment.[16] Earlier, α-TOS has been reported to possess typical anticancer property against multiple cancer cells. We expect that when the lipophilic portion of TOS is conjugated with Pluronic, it would allow better drug solubilization and improve the systemic stability.

Department of General Surgery, The First Affiliated Hospital, China Medical University, Shenyang, Liaoning 110001, China. E-mail: liyuji182@gmail.com

The high drug encapsulation and improved systemic stability might improve the cancer cell mortality.[17,18]

Doxorubicin (DOX), an anthracycline anticancer drug, is indicated in the treatment of multiple cancers including breast, ovarian, prostate, and advanced or recurrent liver cancers.[19] Despite its potent therapeutic effect, clinical application of DOX is hindered by its high toxicity towards normal tissue and severe side effects, such as cardiotoxicity. In this study, therefore, an alternative attempt was made to improve the chemotherapeutic efficacy of DOX and, at the same time, reduce its side effects.[20,21]

In this study, the amine group of Pluronic 123 was chemically conjugated with the carboxylic group of TOS in the terminal portion. We developed the Pluronic/TOS-based polymeric micelles to increase the intracellular concentration of DOX in liver cancer cells. The main goal of this study is to improve chemotherapy towards liver cancers. The DOX-loaded polymeric micelles were prepared by the self-assembly of P/TOS and anticancer drugs. Physicochemical characterizations were performed to ascertain their size and shape parameters. The cytotoxic effect of P/TOS-DOX was studied against HepG2 liver cancer cells. The cellular uptake and intracellular localization of P/TOS-DOX was studied by means of flow cytometer and confocal microscopy. Biodistribution of the drug-loaded polymeric micelles was studied in tumor model to ascertain the concentration of drugs in the vital organs. Finally, *in vivo* anticancer efficacy study was performed in HepG2 cancer cell-bearing, tumor-xenografted nude mice.

Results and discussion

Preparation of self-assembled polymeric micelles

The encapsulation of anticancer drugs in polymeric micelles could not only improves the solubility of drugs, but also decreases the drug-related side effects. In the present study, PEO–PPO–PEO block copolymer (Pluronic) was conjugated with tocopheryl succinate (TOS) to improve drug solubilization and

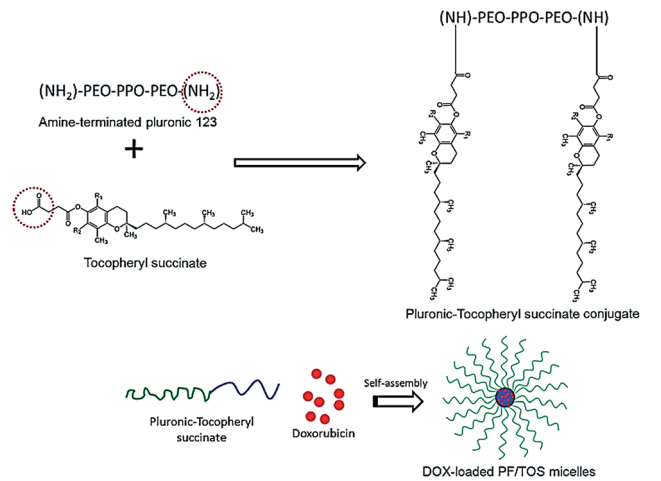

Fig. 1 Schematic illustration of the preparation of Pluronic–tocopheryl succinate block copolymer and the formation of doxorubicin-loaded polymeric micelles.

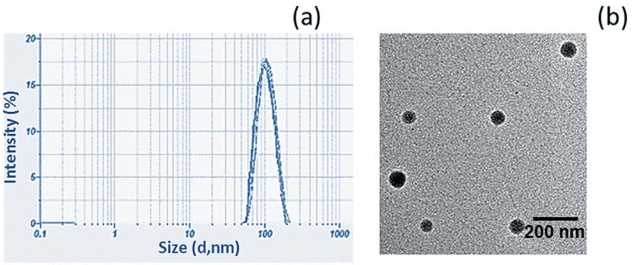

Fig. 2 (a) Size distribution of P/TOS-DOX micelles determined by dynamic light scattering technique, (b) transmission electron micrograph of P/TOS-DOX micelles.

systemic stability (Fig. 1). The micelles stably protect the drug in systemic circulation and control its release.

The P/TOS-DOX micelles were formed by self-assembly. The block copolymer and DOX base spontaneously self-aggregated to form drug-loaded, polymeric micelles. Various inter- and intra-molecular physical forces were involved during the formation of micelles. The core of the polymer micellar delivery system serves as a reservoir that accommodates drug molecules through a combination of hydrophobic and electrostatic interactions, hydrogen bonding, or chemical conjugation of the drug to the core-forming block of the copolymer. The P-TOS conjugate, composed of hydrophilic PEO and hydrophobic tocopheryl succinate, self-aggregates in the aqueous media to form typical core–shell nanoparticles. The critical micellar concentration (CMC) of the so-formed P/TOS-DOX micelles is 25 μg ml^{-1}. The average size of P/TOS-DOX was found to be around ~100 nm, with an excellent dispersity index of 0.15 (PDI) (Fig. 2a). Particle size has been reported to be an important requirement for biodistribution and long blood circulation time. Additionally, smaller particles (<200 nm) could evade phagocytosis and passively target cancer tissues *via* the enhanced permeation retention (EPR) effect.[22] The particle size was further confirmed in the dried state by means of TEM imaging. The particles were spherical in nature, with a perfect boundary surrounding each particle (~80 nm). The particles were uniformly dispersed in the copper grid (Fig. 2b). Moreover, the size of the nanoparticles measured from TEM was consistent with the DLS observation, although the state of the particles was different in these two methods.

The drug loading capacity (LC) of the NPs was evaluated in order to demonstrate its suitability for systemic administration. The LC of P/TOS-DOX was observed to be 21.2 ± 2.65%, indicating its ability to retain a high amount of the drug in the micelle core. In contrast, Pluronic–DOX showed a very low LC of 8.5 ± 3.1% due to the lack of sufficient hydrophobicity.

In vitro drug release

The release of DOX from P/TOS-DOX micelles was studied in three different pH conditions (pH 7.4, pH 6.8, and pH 5.0). As demonstrated in Fig. 4, micelles showed a typical pH-responsive drug release pattern, with a high release rate in lower, acidic pH levels. It can be seen that nearly ~15%, ~28%, and ~50% of DOX was released at pH 7.4, pH 6.8, and pH 5.0, respectively. By

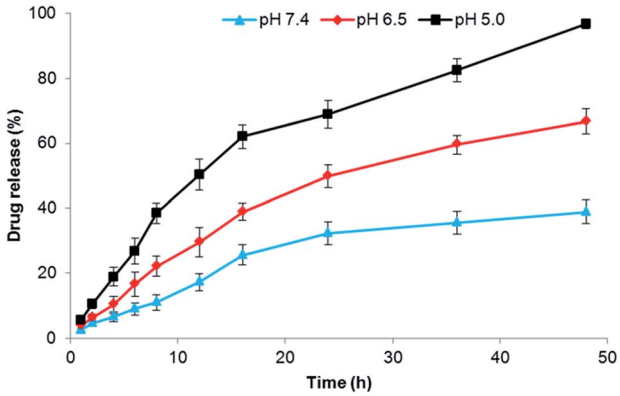

Fig. 3 *In vitro* release profile of DOX from P/TOS-DOX micelles. The release study was performed in pH 7.4, pH 6.8, and pH 5.0 conditions. Results are expressed as means + standard deviation from three independent experiments.

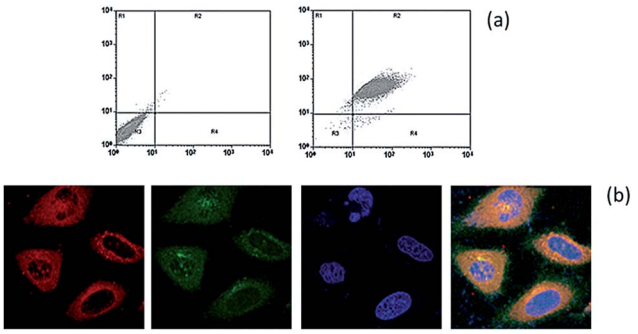

Fig. 4 (a) Qualitative cellular uptake analysis of P/TOS-DOX micelles in HepG2 cancer cells. Fluorescence visualization was carried out using confocal laser scanning microscopy. The concentration of DOX used was 10 μg ml^{-1}. (b) Flow cytometer analysis of P/TOS-DOX micelles after 3 h incubation.

48 h, almost 100% of the drug was released at pH 5.0, whereas >60% of the drug is still entrapped in the micelles at pH 7.4 (Fig. 3). As clearly seen in Fig. 3, a higher DOX release rate was achieved at lower pH using the present system. The basic nature of doxorubicin ($pK_a = 8.3$) gives it higher solubility at lower pH. Therefore, DOX entrapped in the micelles has a greater tendency to go into the release medium of lower pH. The favored release in acidic medium would result in a higher release rate of doxorubicin in tumor cells, adding therapeutic efficiency to the delivery system. It is worth noting that no initial release burst of the drug was observed in any pH condition, indicating that the drug was well incorporated in the hydrophobic core of the micelles.[23] The particle size of P/TOS-DOX micelles after 1 h of release study was observed to be ~110 nm, while the size decreased to ~70 nm after 24 h of the release study. The decrease in particle size of micelles could be due to the release of the drug from the bulkier core of the system. Overall, a sustained release of DOX was observed from the micelles, which may be due to better solubilization of the drug in the hydrophobic core. Such sustained and controlled release of the anticancer drug might be advantageous in cancer targeting.

Cellular uptake

Confocal laser scanning microscope was used to study the cellular uptake mechanism of P/TOS-DOX in HepG2 cancer cells. To visualize the cellular uptake and associated mechanisms, lysosomes were stained with Lysotracker green, and nuclei were stained with DAPI. The confocal microscopy images show that red fluorescence (originating from P/TOS-DOX) was mainly located in the cytoplasmic region rather than the entire cell (Fig. 4a). The high intensity of DOX fluorescence in the perinuclear region suggests that much of the drug was released from the micelles and is available in the free form. It is expected that the acidic conditions in the lysosome provoked the release of DOX from the micellar delivery systems. These results corroborate the fact that micelles, after endocytosis uptake, destabilize in the cytoplasmic region, resulting in the release of the drug, which then travels to the nuclear region. It has been reported by many authors that micelles release the therapeutic load in the cytosol and perinuclear region of cells.[24,25]

Flow cytometer analysis was carried out to quantitate the micelle internalization. The flow cytometer sorting showed that cells were predominantly present in the double-positive chamber (quadrant), whereas control cells were largely present in the lower quadrant (Fig. 4b). The results therefore clearly suggest that micelles were present in the cytoplasmic region, consistent with the confocal microscopy images. The distribution of micelles in the cytoplasmic region will improve the cancer-killing potency of the chemotherapeutic drug.

Cytotoxic effect of blank and drug-loaded micelles

The biocompatibility and cytotoxic effect of polymeric micelles was evaluated by means of MTT assay. The biocompatibility of nanomaterials employed as delivery carrier is of utmost importance in ensuring the high success rate of the cancer delivery system. The blank micelles were exposed to HepG2 cancer cells at different concentrations, to a maximum of 100 μg ml^{-1}. It was observed that micelles maintained an excellent biocompatibility profile throughout all the concentrations tested. Especially, >90% cell viability was observed in cells exposed to 100 μg ml^{-1} micelles for 24 h (Fig. 5a). The results therefore suggest that the block polymers as well as the micelles are safe and could be potentially used for systemic targeting.

The anticancer effect of drug-loaded micelles was studied in order to evaluate their suitability as efficient carriers in liver cancer treatment. The cytotoxic effect of DOX and P/TOS-DOX was studied in HepG2 cancer cells. As shown in Fig. 5b, DOX and P/TOS-DOX showed a typical concentration-dependent cytotoxicity, whereas drug-loaded micelles showed superior cytotoxic effect compared to that of free DOX. The IC_{50} value was calculated to estimate its cytotoxic effect. The IC_{50} value of DOX and P/TOS-DOX remained at 1.18 μg ml^{-1} and 0.72 μg ml^{-1}, respectively, indicating the significant inhibition of cancer cell proliferation by the micellar carrier system. The difference in the cytotoxic effect of the free drug and the drug-loaded carrier

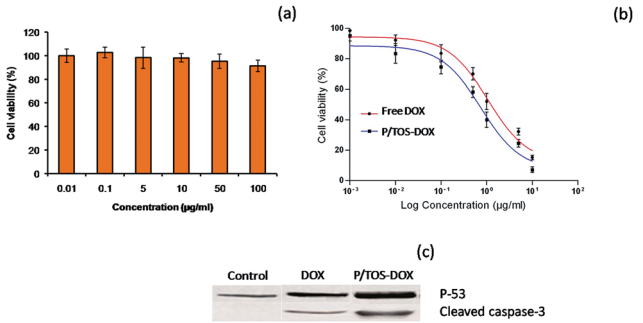

Fig. 5 (a) Biocompatibility profile of P/TOS blank polymeric micelles studied against HepG2 cancer cells. (b) Cell viability of HepG2 cancer cells upon incubation with free DOX and P/TOS-DOX micelles after 24 h incubation. The cell cytotoxicity was evaluated by means of MTT assay.

might be due to the nature of cellular uptake and intracellular mechanisms. It has been reported that free DOX, due to its small molecular weight and hydrophilic nature, could directly diffuse into the cancer cell and, simultaneously, be pumped out. In the case of P/TOS-DOX, endocytosis-mediated cellular uptake might allow the slow and continuous drug release in the intracellular environment, resulting in higher cell cytotoxicity and cell death.[26] DOX localized in the cell nuclei likely intercalates into DNA strands, thus showing its toxicity against tumor cells.

The over-expression of P53 and caspase-3 is regarded as the hallmark of cell apoptosis, or cancer cell death. These apoptosis markers are highly expressed in tumor-suppressive conditions. The result was consistent with the cytotoxic assay, as the nanoformulations showed high expression of both P53 and caspase-3 (Fig. 5c).

In vivo biodistribution studies

The biodistribution of free DOX and P/TOS-DOX was studied in the HepG2 cancer cell-bearing tumor model. It can be seen that both free DOX and P/TOS-DOX attained high concentrations in blood after 1 h of intravenous administration, while less than 2% of free drug was detected at the end of the study period. On the other hand, drug-loaded micelles maintained a significantly higher concentration even at the end of 24 h (Fig. 6a and b). The data clearly reflect that micellar incorporation of the drug effectively shielded it from elimination, and subsequently prolonged the blood circulation and half-life of the anticancer drug. Such prolonged blood circulation profile will effectively facilitate the passive targeting of the drug in the tumor tissues *via* EPR effect. Subsequently, P/TOS-DOX accumulated preferentially in the tumor immediately after systemic administration, and a significant proportion of the drug was observed by the end of 24 h. Meanwhile, only ~5% of the drug could be found in tumors of the free drug-administered group after 1 h, and no drug was found after 24 h, indicating the rapid elimination of drug from the systemic circulation. One more observation from the biodistribution study is that nearly ~15% of DOX was observed in heart following the administration of the free drug, and a significant level was still present by the end of 24 h. On the contrary, less than <5% of the drug accumulated in the heart tissue from P/TOS-DOX, indicating its safety profile. The biodistribution profile clearly suggests that the micellar carrier extended the blood circulation profile, while at the same time reduced organ-related toxicity.

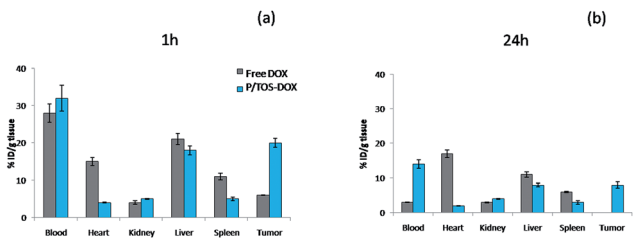

Fig. 6 Biodistribution profile of DOX from P/TOS-DOX micelles after intravenous administration to tumor-bearing nude mice after (a) 1 h and (b) 24 h. The formulations were administered *via* tail vein injection.

Antitumor efficacy studies

The *in vivo* antitumor study was performed in the HepG2 hepatic cancer cell-bearing tumor mouse model. An antitumor efficacy study was carried out to evaluate the effect of the micellar carrier on the tumor suppression rate. As shown in Fig. 7a, tumor volume rapidly increased in the control group, reaching over 2500 mm^3 at the end of the 18th day. The free DOX and P/TOS-DOX treated groups showed effectively suppressed tumor growth. Especially, P/TOS-DOX exhibited superior tumor growth inhibition compared to that of the free DOX treated group. On day 18, the free DOX treated group showed a tumor volume of ~1200 mm^3, whereas the P/TOS-DOX treated group showed a tumor volume of only ~600 mm^3. A combination of multiple factors could explain the superior antitumor effect of P/TOS-DOX in tumor mice. Especially, the prolonged blood circulation profile of P/TOS-DOX effectively facilitated passive tumor targeting *via* the EPR effect. The passive targeting of micelles might increase the intracellular concentration of

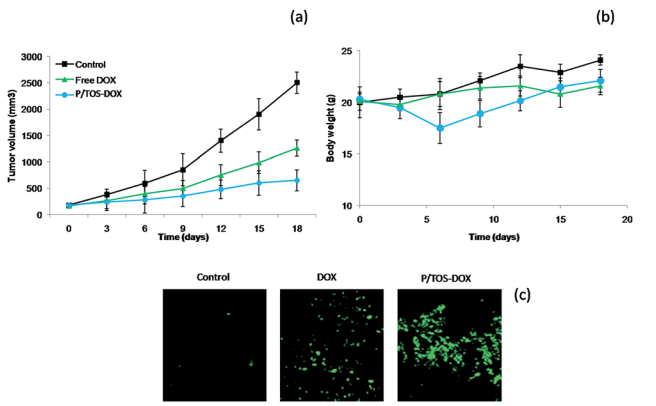

Fig. 7 *In vivo* antitumor efficacy evaluation in the HepG2 tumor-bearing mouse model treated with free DOX and P/TOS-DOX micelles. An untreated mice group was observed as control. (a) Tumor volume variations, (b) variation of body weight, (c) TUNEL assay of the extracted tumor section.

anticancer drugs. Moreover, a pH-responsive release pattern of P/TOS-DOX might trigger drug liberation at the target site in the nucleus.[27]

Body weight was monitored to observe the safety profile of the administered formulations. As seen from Fig. 7b, the free DOX treated group lost more than 10% of body weight, indicating its severe systemic toxicity. The P/TOS-DOX treated group, however, did not show any sign of weight loss, indicating its excellent safety profile.

The anticancer efficacy of the formulation was further studied by means of TUNEL assay (Fig. 7c). The P/TOS-DOX treated group showed significantly higher TUNEL-positive tumor cells, indicating the superior apoptosis effect of micellar carriers. The data clearly reflect that drug-loaded micellar formulations remarkably increased apoptosis in cells and decreased the number of proliferating tumor cells.

Conclusion

In conclusion, doxorubicin-loaded Pluronic-alpha-tocopheryl succinate polymeric micelles (P/TOS-DOX) were successfully prepared towards the therapeutic treatment of hepatocellular carcinoma. We have shown that drug-loaded micelles exhibit a typical pH-dependent and sustained drug release profile. These micelles were nanosized, around ~100 nm, with spherical morphology. The micelles were predominantly distributed in the cytoplasmic region, which facilitates the cancer-killing potency of the chemotherapeutic drug. The IC_{50} value of DOX and P/TOS-DOX remained at 1.18 μg ml^{-1} and 0.72 μg ml^{-1}, respectively, indicating the significant inhibition of cancer cell proliferation by the micellar carrier. Subsequently, micellar incorporation of the drug effectively shielded it from elimination and subsequently prolonged the blood circulation and half-life of the anticancer drug. P/TOS-DOX accumulated preferentially in the tumor immediately after systemic administration, and a significant proportion of the drug was observed by the end of 24 h. Especially, P/TOS-DOX exhibited superior tumor growth inhibition compared to that of the free DOX treated group. More importantly, the side effects of DOX were effectively decreased by the administration of micellar carriers. Overall, our results suggest that P/TOS-DOX could be an attractive carrier in the therapeutic approach to hepatocellular carcinoma.

Materials and methods

Materials

Pluronic P 123, tocopheryl succinate, and 1-(3-dimethyl aminopropyl)-3-ethylcarbodiimide hydrochloride (EDC·HCl) were purchased from Sigma-Aldrich, China. Doxorubicin hydrochloride was procured from Zhejiang Hisun Pharmaceutical Co., Ltd. (Taizhou, China). Unless otherwise stated, all other chemicals were reagent grade and used without further purification.

Preparation of doxorubicin-loaded Pluronic 123-tocopheryl succinate micelles

Pluronic 123 was conjugated with tocopheryl succinate as reported earlier.[28] Briefly, the amino group of Pluronic 123 (P123) was chemically conjugated with the carboxyl group of tocopheryl succinate (TOC). For this, 500 mg of P123 (amine-terminated), 76 mg of TOC, and 108 mg of EDC were dissolved in 5 ml of DMSO. The entire mixture was stirred in an inert atmosphere for 40 h. The resulting chemical conjugate was dialyzed (MW 3000 cut-off) using a dialysis bag for 1 week with frequent replacement of distilled water. By this process, unreacted or unconjugated TOC or P123 was removed, and the final product was carefully freeze-dried.

Prior to the preparation of drug-loaded micelles, doxorubicin·HCL (DOX) was converted into the base form by the addition of excess trimethylamine. The DOX base was used for the subsequent entrapment process. 5 mg of DOX and 50 mg of P123–TOS conjugate (P/TOS) were dissolved in acetonitrile and stirred for 1 h. The organic mixture was then packed in a dialysis bag and dialyzed against distilled water for 12–24 h. The organic solvent and un-entrapped DOX were removed by dialysis bag, and the final DOX-loaded P/TOS (P/TOS-DOX) was collected, freeze-dried, and used for further experiments.

Characterization of P/TOC-DOX micelles

The surface charge, hydrodynamic diameter, and distribution index of P/TOC-DOX were evaluated by dynamic light scattering technique. Malvern Zetasizer Nano ZS (UK) was used to determine the size and charge of the micelles. The samples were suitably diluted with distilled water and analyzed at a fixed angle of 173° at 25 °C.

The morphology of micelles was determined by means of transmission electron microscope (TEM; JEOL, Japan). A dilute solution was prepared and dropped onto a carbon-coated copper grid. The samples were then stained with phosphotungstic acid (PTA) and allowed to stay for 15 min. The samples were then dried and observed under TEM.

Evaluation of drug content

The entrapment efficiency (EE) and drug loading capacity (DLC) were estimated by spectroscopy. Briefly, DOX-loaded micelles (freeze dried) were dissolved in water, and methanol was added in the ratio of 1/50 fold. The mixture was centrifuged, and the supernatant was evaluated for the amount of DOX incorporated. The amount of DOX was quantified by UV-vis spectroscopy at 482 nm. EE and DLC were calculated using the following formulas:

$$\text{EE (\%)} = (\text{amount of DOX entrapped} / \text{total DOX added initially}) \times 100$$

$$\text{DLC (\%)} = (\text{amount of DOX entrapped} / \text{total weight of nanoparticles}) \times 100$$

In vitro drug release

The drug release study was carried out using the dialysis method. For this purpose, freeze-dried, drug-loaded polymeric micelles were dissolved in a measured quantity of distilled water such that the final concentration remained at 1 mg ml^{-1} of dispersion. 1 ml of nanoparticle dispersion was placed in the dialysis membrane (MW 3500 Da), and both ends were tightly sealed. The dispersion-loaded dialysis membrane was immersed in a Falcon tube containing 25 ml of release media. Phosphate buffered saline (PBS, pH 7.4) and acetate buffered saline (ABS, pH 5.0) were used as respective release media. At specific time points, 1 ml of release medium was withdrawn and replaced with an equal volume of fresh release medium. The amount of drug released in the release media was quantified using UV-vis spectrophotometer at 482 nm.

Cell culture

Human hepatocarcinoma cell line HepG2 was purchased from the Chinese Academy of Science Cell Bank for Type Culture Collection (Shanghai, China). HepG2 cells were cultured in DMEM growth medium supplemented with 10% (v/v) fetal bovine serum (FBS) and 1% penicillin–streptomycin mixture. The cells were maintained at ambient conditions of 5% CO_2/95% air atmosphere at 37 °C.

Cytotoxicity assay

The anticancer effects of free DOX and P/TOS-DOX were tested in HepG2 cancer cells by MTT assay. The cells were grown in fully supplemented DMEM medium and plated in a 96-well plate at a seeding density of 1×10^4 cells per well. Cells were allowed to attach for 20 h, after which they were treated with the respective formulations at different concentrations and further incubated for 24 h. The medium was removed, and cells were washed twice with PBS. Then, 3-(4,5-dimethylthiazol-2-yl)-2,5-diphenyl tetrazoliumbromide (MTT) solution in PBS (20 μl, 5.0 mg ml^{-1}) was added and further incubated for 4 h. The supernatant was carefully removed, and formazan was extracted by means of DMSO (100 μl). The absorbance was measured at 490 nm using a microplate reader. The cell viability was compared with control cells, which were untreated. The cytotoxicity of bare polymeric micelles (without the drug) was investigated in the same manner.

Flow cytometric analysis

The cells were seeded in a 6-well plate and allowed to attach for 20 h. The cells were treated with P/TOS-DOX and incubated for 4 h. The cells were extracted by means of 0.25% trypsin. The cell suspension was centrifuged, washed twice, and reconstituted in PBS. The cellular uptake was observed in a BD FACSCalibur flow cytometer (Beckton Dickinson, U.S.A.) and analyzed using Cell Quest software.

Cellular uptake by confocal microscopy

The cellular uptake of P/TOC-DOX micelles was further studied by confocal microscopy. Briefly, HepG2 cells were added to the 6-well plate at a seeding density of 1×10^5 cells per well and incubated for 24 h. The cells were then exposed to P/TOC-DOX micelles and incubated for 3 h at 37 °C. The medium was removed, and cells were carefully washed twice with PBS. The lysosome was stained with Lysotracker Green, and nuclei were stained with DAPI. Cells were again washed and fixed with 4% (w/v) paraformaldehyde. The samples (cover slips) were then observed under confocal microscope. Confocal laser scanning microscopy was performed on a Leica TCS SP5 II equipped with a 63× oil immersion objective lens.

In vivo antitumor study

The *in vivo* antitumor study was carried out in human liver hepatocellular carcinoma (HepG2) tumor cell-bearing nude mice. The xenograft model was created by injecting HepG2 cell suspension (1×10^6) into the right flank of 5 week old nude mice. The experiments were started when the tumor volume reached approximately ~100 mm^3. Following this, mice were divided into 3 groups, with 8 mice in each group. Each group received DOX and P/TOS-DOX at an equivalent dose of 5 mg kg^{-1}, and the third group was maintained as control. The tail vein injections were carried out 3 times at an interval of 3 days. The tumor volume and body weight of mice were monitored during the entire study period. Specifically, tumor volume was measured using a Vernier caliper, and the tumor size was calculated using the equations: $V = a \times b^2/2$, where '*a*' and '*b*' represent the longest and shortest diameters.

In vivo TUNEL assay

After the antitumor study, tumors were surgically removed, fixed with 10% formalin, and kept at 4 °C. TUNEL assay was performed following the manufacturer's cell death detection kit protocol (Roche, Mannheim, Germany). The sections were placed in the glass slide and deparaffinized, and proteinase K was added to the slides. The slide was incubated for 40 min, rinsed twice with PBS, and then incubated with TUNEL reaction mixture for a further 45 min. The slides were washed and incubated with the reaction mixture (50 μl TUNEL reaction mixture + 2 μl enzyme solution + 48 μl label solution). The slides were washed and viewed under confocal laser scanning microscope (Leica TCS SP5 II equipped with a 63× oil immersion objective lens). The extent of green fluorescence was interpreted in terms of apoptotic cells.

Biodistribution study

For the biodistribution study, the tumor model was developed as mentioned in the above section. The xenograft model was created by injecting HepG2 cell suspension (1×10^6) into the right flank of the 5 week old nude mice. The experiments were started when the tumor volume reached approximately ~100 mm^3. Each mice group was administered with DOX and P/TOS-DOX *via* tail vein injections. Specific animals were selected at 1 h and 24 h of experimental time. Animals were given a high dose of ketamine/xylazine (100 mg kg^{-1} and 10 mg kg^{-1}, respectively) IP to induce anesthesia. Then, blood was collected, heparinized, and stored. Individual organs,

including tumor, liver, spleen, kidney, and heart were collected and washed quickly with PBS. The organs were collected in pre-weighed EP tubes and assayed for DOX content. 1 ml of PBS was added to the pre-weighed organs, and these were sonicated using 30 cycles of Bioruptor ultrasonic treatment, active every 15 s for a 15 s duration at 200 W, in an ice bath. The homogenate was processed by the abovementioned extraction process for sample preparation, and the amount of drug in each organ was estimated by means of HPLC.

Statistical analysis

Data are presented as mean + SD. Differences between more than two groups were assessed by one-way ANOVA using SPSS 17.0.

Acknowledgements

This work was supported by the research grant of China Medical University, China.

Notes and references

1 R. Siegel, C. DeSantis and K. Virgo, *et al.*, *Ca-Cancer J. Clin.*, 2012, **62**, 220.
2 M. Marra, I. M. Sordelli and A. Lombardi, *et al.*, *J. Transl. Med.*, 2011, **9**, 171.
3 M. Caraglia, G. Giuberti and M. Marra, *et al.*, *Cell Death Dis.*, 2011, **2**, 150.
4 G. J. Kim and S. Nie, *Mater. Today*, 2005, **8**, 28.
5 R. K. Jain, *J. Controlled Release*, 1998, **53**, 49.
6 J. L. S. Au, S. H. Jang, J. Zheng, C. T. Chen, S. Song, L. Hu and M. G. Wientjes, *J. Controlled Release*, 2001, **74**, 31.
7 M. L. Etheridge, S. A. Campbell, A. G. Erdman, C. L. Haynes, S. M. Wolf and J. McCullough, *Nanomedicine*, 2013, **9**, 1.
8 V. P. Torchilin, *Nat. Rev. Drug Discovery*, 2005, **4**, 145.
9 K. Kataoka, A. Harada and Y. Nagasaki, *Adv. Drug Delivery Rev.*, 2001, **47**, 113.
10 H. Maeda, *Bioconjugate Chem.*, 2010, **21**, 797.
11 N. Suthiwangcharoen, T. Li, L. Wu, H. B. Reno, P. Thompson and Q. Wang, *Biomacromolecules*, 2014, **15**, 948.
12 T. Li, L. Wu, N. Suthiwangcharoen, M. A. Bruckman, D. Cash, J. S. Hudson, S. Ghoshroy and Q. Wang, *Chem. Commun.*, 2009, 2869.
13 Z. Wei, S. Yuan, Y. Z. Chen, S. Y. Yu, J. G. Hao, J. Q. Luo, X. Y. Sha and X. L. Fang, *Eur. J. Pharm. Biopharm.*, 2010, **75**, 341.
14 A. V. Kabanov, E. V. Batrakova and V. Y. Alakhov, *Adv. Drug Delivery Rev.*, 2002, **54**, 759.
15 W. Zhang, Y. Shi, Y. Chen, J. Ye, X. Sha and X. Fang, *Biomaterials*, 2011, **32**, 2894.
16 M. Birringer, J. H. EyTina, B. A. Salvatore and J. Neuzil, *Br. J. Cancer*, 2003, **88**, 1948.
17 J. Neuzil, *Br. J. Cancer*, 2003, **89**, 1822.
18 Y. W. Won, S. M. Yoon, C. H. Sonn, K. M. Lee and Y. H. Kim, *ACS Nano*, 2011, **5**, 3839.
19 V. Voliani, G. Signore, O. Vittorio, P. Faraci, S. Luin, J. Perér-Prieto and F. Beltram, *J. Mater. Chem. B*, 2013, **1**, 4225.
20 D. G. Ahn, J. Lee, S. Y. Park, Y. J. Kwark and K. Y. Lee, *ACS Appl. Mater. Interfaces*, 2014, **6**, 22069.
21 N. Suthiwangcharoen, T. Li, K. Li, P. Thompson, S. You and Q. Wang, *Nano Res.*, 2011, **5**, 483.
22 V. P. Torchilin, *Eur. J. Pharm. Biopharm.*, 2009, **71**, 431.
23 H. Yuan, L. J. Lu, Y. Z. Du and F. Q. Hu, *Mol. Pharm.*, 2011, **8**, 225.
24 T. Ramasamy, H. B. Ruttala, J. Y. Choi, T. H. Tran, J. H. Kim, S. K. Ku, H. G. Choi, C. S. Yong and J. O. Kim, *Chem. Commun.*, 2015, **51**, 5758–5761.
25 J. L. Markman, A. Rekechenetskiy, E. Holler and J. Y. Ljubimova, *Adv. Drug Delivery Rev.*, 2013, **65**, 1866.
26 Q. Tian, X. H. Wang, W. Wang, C. N. Zhang, P. Wang and Z. Yuan, *Nanomedicine*, 2012, **8**, 870.
27 D. E. Owens III and N. A. Peppas, *Int. J. Pharm.*, 2006, **307**, 93.
28 V. Saxena and M. D. Hussain, *Int. J. Nanomed.*, 2012, **7**, 713–721.